

# The antimatter spectrometer (AMS-02): A particle physics detector in space

Roberto Battiston<sup>1</sup>

*Physics Department and INFN Section, Perugia 06123, Italy*

On behalf of the AMS-02 Collaboration  
Available online 15 January 2008

## Abstract

Antimatter spectrometer (AMS)-02 is a spaceborne magnetic spectrometer designed to measure with accuracies up to one part in  $10^9$  the composition of cosmic rays near the Earth. With a large acceptance ( $5000 \text{ cm}^2 \text{ sr}$ ), an intense magnetic field from a superconducting magnet (0.7 T) and an accurate particle identifications AMS-02 will provide the highest accuracy in cosmic rays measurements up to the TeV region. During a 3-year long mission on the International Space Station (ISS) AMS-02 will achieve a sensitivity to the existence of anti-He in the cosmic rays of one part in a billion as well as important informations on the origin of Dark Matter. We review the status of the construction of the AMS-02 experiment in preparation for the 3-year mission on the ISS.

© 2008 Elsevier B.V. All rights reserved.

PACS: 13.85.Tp; 29.30.Aj; 95.85.Ry; 96.40.De

Keywords: Space cosmic rays; Cosmic-ray antiprotons; Superconducting spectrometers

## 1. Introduction

Antimatter spectrometer (AMS) is a particle physics experiment in space. The purpose is to perform accurate, high-statistics, long-duration measurements of the spectra of energetic (up to multi-TeV) primary cosmic rays in space. Some of the physics goals are:

- *Dark matter*: There are many theoretical suggestions [1] that particles predicted by SUSY theories, for example the neutralino  $\chi$ , are a component of the dark matter, which constitutes one-quarter of the mass of the universe. Collisions of dark matter in the galactic halo produce  $\bar{p}$ ,  $e^+$  and  $\gamma$  via:

$$\begin{aligned}\chi + \chi &\rightarrow \bar{p} + \dots \\ &\rightarrow e^+ + \dots \\ &\rightarrow \gamma + \dots\end{aligned}$$

*E-mail address:* [r.battiston@tiscali.it](mailto:r.battiston@tiscali.it)

<sup>1</sup>Work partially supported by the grant I/021/05/0 of the Italian Space Agency (ASI).

The  $\bar{p}$ ,  $e^+$  and  $\gamma$  from these collisions will produce deviations from the smooth energy spectra. Therefore, the precision measurement of the  $\bar{p}$ ,  $e^+$  and  $\gamma$  spectra will enable AMS to establish whether SUSY particles are the origin of dark matter. There are also predictions that antideuterons can be produced from the collision of SUSY particles, at a level which AMS could detect [2].

- *Antimatter*: The strong evidence that supports the Big Bang theory of the origin of the universe requires matter and antimatter to be equally abundant at the very hot beginning [3]. The absence of sharp annihilation  $\gamma$ -ray peaks excludes the presence of large quantities of antimatter within our local super cluster of galaxies. However there is no direct experimental evidence regarding the remainder ( $10^8$ ) of the universe.
- *Cosmic rays*: AMS will collect  $\sim 10^9$  nuclei and isotopes (D, He, Li, Be, B, C, ..., Fe). Among the interesting issues which will be studied are the accurate determination of the ratio of boron to carbon over a wide range of energies provides crucial information regarding the propagation of cosmic rays in the galaxy. In particular, the ratio of  $^{10}\text{Be}$  (mean lifetime of  $3.6 \times 10^6$  years) to the stable  $^9\text{Be}$  will enable us to extend the low-energy

measurements of the Ulysses satellite to higher energies and to provide important information on the understanding of cosmic ray propagation.

To perform a high-accuracy measurement of the spectra of energetic charged particles in space, the AMS detector is based on experience and observations from experiments to study rare signals among intense backgrounds, such as the study of leptonic decays of vector mesons from  $\gamma + N \rightarrow N + (\rho, \omega, \phi \rightarrow e^+ e^-)$  at DESY [4] and the discovery of the  $J$  particle from  $p + N \rightarrow J(\rightarrow e^+ e^-) + \dots$  [5] combined with the precision measurements made in the study of  $Z$  decays [6]. These experiments were successful because they have:

- (a) minimal material in the particle trajectory so that the material itself is not a source of background nor a source of large-angle nuclear scattering; and
- (b) many repeated measurements of momentum and velocity so as to ensure that background particles which had experienced large-angle nuclear scattering from the detector itself be swept away by the spectrometer and not confused with the signal.

It was the strict adherence to these techniques that ensured that a background rejection of  $10^{10}$  was indeed possible and made these experiments successful. AMS is designed following the same principles. Fig. 1 shows the AMS-02 detector configuration for the International Space Station (ISS).

AMS-02 will contain the following main components:

- (1) a 20-layer Transition Radiation Detector (TRD) which identifies electrons and positrons with a measured rejection factor against hadrons of  $10^3$ – $10^2$  from 1.5 to 300 GeV,
- (2) four layers of time-of-flight (TOF) hodoscopes that provide precision TOF measurements ( $\sim 120$  ps) and  $dE/dX$  measurements,

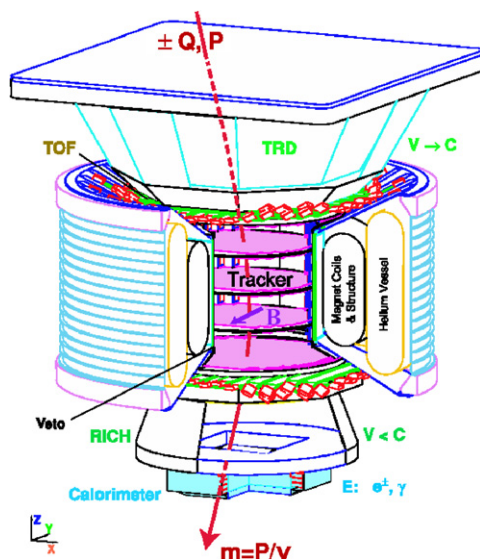


Fig. 1. A TeV detector in space: AMS-02 on the space station.

- (3) the superconducting magnet, which provides a bending power of  $BL^2 = 0.86 \text{ T m}^2$ ,
- (4) eight layers ( $6.45 \text{ m}^2$ ) of silicon tracker, which provide a proton rigidity (= momentum/charge) resolution of 20% at 0.5 TV and a helium (He) resolution of 20% at 1 TV and charge resolution of nuclei up to iron ( $Z = 26$ ),
- (5) veto, or anticoincidence, counters (ACC) which ensure that only particles passing through the magnet aperture will be accepted,
- (6) a ring Imaging Cherenkov Counter (RICH), which measures the velocity (to 0.1%) and charge  $|Z|$  of particles or nuclei. (This information, together with the measurement of momentum in the tracker, will enable AMS to unambiguously determine the mass of these particles and nuclei.)
- (7) a 3-D sampling calorimeter (ECAL) made out of 16.7  $X_0$  (radiation lengths) of lead and scintillating fibres, which measures the energy of gamma rays, electrons and positrons and distinguishes electrons and positrons from hadrons with a rejection of  $10^4$  in the range between 1.5 GeV and 1 TeV,
- (8) a system of two star trackers (AMICA) to allow the precise reconstruction of the origin of high-energy gamma rays reconstructed in the detector.

Due to the limits in the available space, in the following sections we will discuss the characteristics of only two subsystems of the AMS-02 apparatus, the Cryomagnet and the Silicon Tracker, which are at the hearth of the magnetic spectrometer.

## 2. The cryomagnet

The purpose of the superconducting magnet is to extend the energy range of our measurements of particles and nuclei to the multi-TeV region [7]. The magnet design was based on the following technical considerations:

- (i) experience in designing and manufacturing the AMS-01 magnet which was 10 times safer than stress limits allowed,
- (ii) the result of many years of intensive R&D collaboration to design a magnet with the following properties:
  - field configuration identical to the AMS-01 magnet to maintain mechanical stability and follow NASA safety standards;
  - minimized heat loss ( $\sim 100 \text{ mW}$ ) and minimized quench probability.
- (iii) to have the magnet built by experts from the Oxford Instruments R&D group, who have an excellent record in producing highly reliable magnets running in persistent mode without quench. (This group has produced the 8 OSCAR magnets (2.36 T) used in cyclotrons in Japan and England and which have operated for close to 30 years without any quench. This group also built the CLEO magnet at CORNELL

and the CLAS torus at Jefferson Laboratory and the KLOE magnet in Frascati. All are large, high-field, special-purpose magnets which have operated for years without quench. To ensure that these experts are able to devote all their efforts to the construction of the AMS-02 magnet, we have supported a new company, Space Cryomagnetics Ltd., entirely staffed by the experts of the Oxford Instruments R&D group and entirely dedicated to the AMS-02 magnet.)

Two magnets are being built. One is the flight magnet and the other is used for space qualification tests. The magnet has no magnetic field during the shuttle launch and landing, and so there is no force among the coils. Hence for the test magnet the coils are replaced by mass equivalents.

The magnet system, as shown in Fig. 2, consists of superconducting coils, a superfluid helium vessel and a cryogenic system, all enclosed in a vacuum tank. Outside of the vacuum tank are supporting electronics, located in the Cryomagnet Avionics Box (CAB), valves and cabling. The vacuum tank is toroidal with inner diameter 1.1 m, outer diameter 2.7 m and length of the central cylinder surrounding the tracker 0.9 m. The magnet operates at a temperature 1.8 K, cooled by superfluid helium stored in the vessel. It is launched at the operating temperature, with the vessel full of 2500 l of superfluid helium. The magnet will be launched with no field. It will be charged only after installation on the ISS. Because of parasitic heat loads, the helium will gradually boil away throughout the lifetime of the experiment. After the project time of 3–5 years, the helium will be used up and the magnet will warm up and no longer be operable.

The coil system consists of a set of 14 superconducting coils arranged, as shown in Fig. 2, around the inner cylinder of the vacuum tank. The coil set has been designed to give the maximum field in the appropriate direction inside the bore tube, while minimizing the stray field outside the magnet.

The single large pair of coils generates the magnetic dipole field perpendicular to the experiment axis. The 12

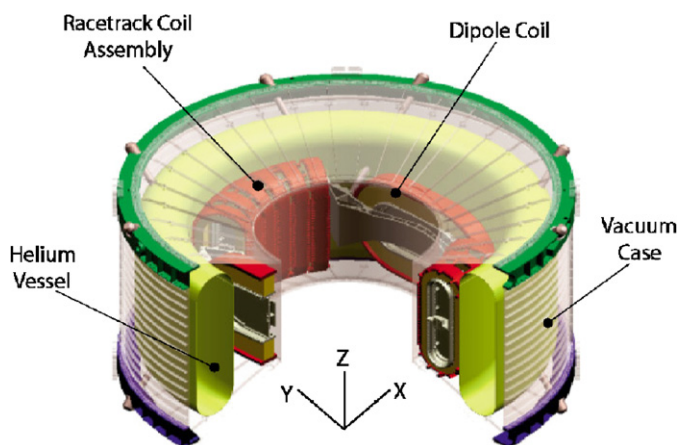


Fig. 2. AMS-02 superconducting magnet layout.

Table 1  
AMS-02 cryomagnet parameters

Central magnetic field $B_x(0,0)$ (T)	0.860
Dipole bending power ( $Tm^2$ )	0.862
Maximum stray magnetic field at $R = 2.3$ m (mT)	15.2
Maximum stray magnetic field at $Y = 2.3$ m (mT)	7.6
Maximum stray magnetic field at $R = 3.0$ m (mT)	3.9
Peak magnetic field on the dipole coils (T)	6.59
Peak magnetic field on the racetrack coils (T)	5.91
Maximum torque in geomagnetic field (Nm)	0.272
Nominal operating magnet current (A)	459.5
Stored energy (MJ)	5.15
Nominal magnet inductance (H)	48

smaller flux return coils control the stray field and, with this geometry, they also contribute to the useful dipole field. The magnetic flux density at the geometric centre of the system is 0.86 T. Table 1 summarizes some of the magnet parameters.

The superconducting wire was developed specifically to meet the requirements of the AMS cryomagnet [1]. The current is carried by tiny ( $22.4\mu m$  diameter) filaments of niobium titanium (NbTi) which—given the magnetic flux and current densities within the coils—carries the current without resistance provided the temperature is kept below 4.0 K. Because pure NbTi has rather low thermal conductivity, it is prone to instability. This can be overcome if it is in intimate contact with a material which has a high thermal conductivity at the cryogenic operating temperature, such as a pure metal. For this reason, the NbTi filaments are embedded in a copper matrix, which is encased in high-purity aluminium. The copper is required for manufacturing reasons, but the aluminium is extremely conductive and much less dense, thus providing maximum thermal stability for aluminium weight. The diameter of the round copper strand at the centre is 0.76 mm, and the aluminium dimensions are  $2.0\text{ mm} \times 1.5\text{ mm}$ . The current density in the superconductor is 2300 or  $157\text{ A/mm}^2$  including the aluminium.

To manufacture the coils, the superconducting wire was first cleaned then insulated using  $85\mu m$  thick polyester tape. Each coil was wound separately onto an aluminium former from a single length of conductor before being impregnated under vacuum with epoxy resin. The impregnation process gives the coils mechanical integrity, and also provides electrical insulation between turns and layers. After completion, each coil is tested individually under conditions as representative as possible of flight, to test the integrity of the design and the quality of the build.

Each of the two larger (dipole) coils, which generate most of the useful field, has 3360 turns, and the 12 smaller (flux return) coils each have 1457 turns. The 14 coils are connected in series, with a single conductor joint between each pair of adjacent coils. The current when the magnet is operating is 459.5 A. All of the coils have been manufactured and tested (see Fig. 3).



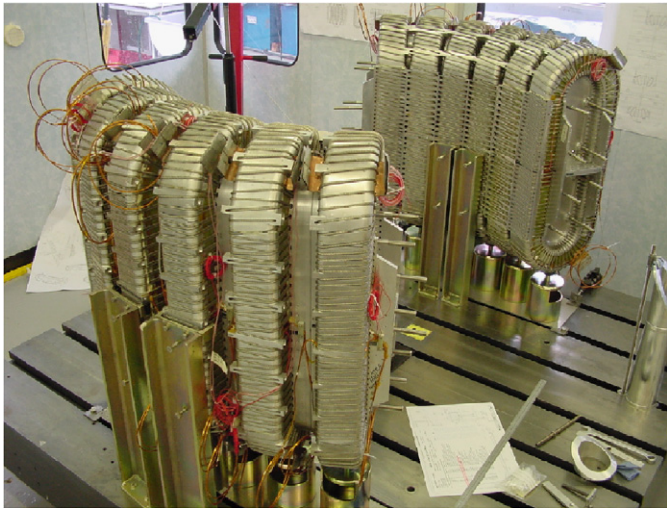


Fig. 3. Coil assembly.

The coils are not coupled thermally. This means that a quench in one coil, leading to a rise in temperature, will not necessarily propagate to any of the others. If this was allowed to happen, the entire stored energy of the magnet (5MJ) could be dissipated as heat in the coil which quenched. While the temperatures reached in that coil would not be dangerous, sufficient thermal stresses could be induced (by differential thermal contraction between parts of the coil) that the performance of the coil might be permanently reduced. For this reason, all the coils are constantly monitored by an electronic protection system. If the onset of a quench is detected in any coil, heaters are powered in the other coils to quench all 14 simultaneously. This distributes the stored energy between the coils, preventing any single coil from taking a disproportionate amount of energy which could otherwise result in degradation. The operation of these quench heaters is an important part of the testing and qualification procedure for the magnet coils.

Each coil is subject to internal forces as a result of its own magnetic field. In general, these are burst forces, trying to expand the racetrack-shaped coil into a ring. These loads are in the plane of the coil, and are resisted by the former on which the coil was wound. In addition, each coil is attracted or repelled by all the other coils in the magnet. This leads to a relatively complicated load system on some of the coils, with forces perpendicular to the plane of the coil. The magnetic loads are quite large: the two dipole coils feel a net attraction to each other around 250 tonnes. During individual coil testing, each coil is charged until some part of the winding is subject to the same force it will experience in flight.

The cold mass of the magnet is more than 2000 kg. This has to be supported from the experiment structure (in particular the vacuum tank), which is at ambient temperature ( $\sim 270 \pm 40$  K). The design of the support straps is therefore crucial, as they have to be able to carry the load without conducting significant heat across the

large temperature gradient. Each consists of a pair of composite bands connected in parallel. One band is thin, with low stiffness and strength, and is permanently connected between the cold mass and the vacuum tank. The other band is much thicker and stronger, but possesses a passive disconnect feature. This means that it only forms a thermal path between the vacuum tank and the magnet during launch and landing. At other times (when it is not needed), differential thermal contraction between the bands and the removal of the high inertial load cause the disconnect to open, dramatically reducing the thermal conduction of the support. A total of 16 straps support the magnet from the vacuum tank. During normal operations on the ground or in space, only the low-stiffness band is engaged, and the heat conduction is very low (less than 3 mW per support). During launch, the high-stiffness band engages as well. The conducted heat load is much higher but because the launch takes only a few minutes the effect on the overall endurance of the system is not significant. The dual stiffness characteristic of the straps makes their behaviour non-linear and, as major structural components of the magnet system, they have been subject to special scrutiny and testing, particularly testing to failure, to understand the safety margins.

The cooling of terrestrial superconducting magnets using liquid helium is a well-established technology, but there is much less experience of helium cryogenics in space. The cryogenic system for the AMS magnet combines technologies from terrestrial magnet cryogenics and space cryogenics to meet the particular challenges of the Space Shuttle launch and the environment of the ISS [8]. It maintains the magnet at a temperature of 1.8 K, under all operating conditions, for the duration of the experiment. Liquid helium ( $^4\text{He}$ ) can exist in two forms. Normal liquid helium behaves in a conventional manner. But if it is cooled below 2.17 K, some of its properties change dramatically as it becomes a superfluid. In particular, its viscosity falls almost to zero, and its apparent thermal conductivity increases by many orders of magnitude.

The AMS-02 magnet is cooled by superfluid helium. There are two main reasons for this. Firstly, the specific latent heat and density of superfluid helium are both higher than in normal liquid helium. Since the amount of cryogen that can be carried is limited by the size of the helium vessel, this gives a useful endurance benefit (there is a greater mass of helium, and each kilogram has a higher cooling capability).

Secondly, in zero gravity there can be no convection currents. In normal liquid helium this can result in thermal stratification, making it difficult to ensure that all parts of the system are fully cold. In the superfluid state, however, the very high thermal conductivity makes it impossible for the helium to support large temperature gradients, so the system remains isothermal.

Any large cryogenic vessel has to be viewed as a potential safety hazard, particularly when it is in an enclosed space such as the payload bay of the Space Shuttle. Safety of the

AMS magnet has to be assured in ground handling operations, during launch, on orbit and during landing. All cryogenic volumes, as well as the vacuum tank, are protected by burst discs to prevent excessive pressure building up in any fault conditions. Some of the burst discs have to operate at temperatures below 2 K, and these have been the subject of a special development and testing programme. In addition, extra protection is provided to mitigate the effect of a catastrophic loss of vacuum. This could be caused, during ground handling operations, by a serious rupture of the vacuum case. If the vacuum case had a large puncture, air could rush through the gap and condense on the surface of the helium vessel. This would result in rapid pressurization and venting of the helium in the vessel. To slow down the rates of pressurization and venting (making the pressure relief path smaller and more manageable) a 3 mm layer of lightweight cryogenic insulation will be applied to the outside surface of the helium vessel. Carefully constructed experiments have shown that this insulation reduces the heat flux to the superfluid helium by a factor of 8 following a sudden, total loss of vacuum. All parts of the AMS magnet system are subject to a battery of tests to ensure their quality and integrity, and their suitability for the mission.

Every one of the 14 superconducting coils will have been tested before assembly into the final magnet configuration. All 12 of the flux return coils have been tested successfully, and the first of the two dipole coils is undergoing final preparations for testing. A special test facility has been constructed and it allows the coil to be operated under cryogenic conditions as close as possible to flight. In particular, the coil is mounted in a vacuum space, and is cooled by a thermal bus bar of the same construction as the one in the flight system.

A full-scale replica of the superfluid thermal bus bar system outlined above was designed and assembled. Heaters on the part of the thermal bus bar outside the helium vessel were then used to simulate the heat load due to the magnet coils being charged. Up to 6 W could be generated by the heaters and transferred by Gorter-Mellink conduction through the thermal bus bar to be dissipated in the vessel of boiling helium. If the heaters were used to generate more power, the Gorter-Mellink conduction broke down: the thermal bus bar was unable to transfer the heat and the temperatures within it began to rise rapidly. These results corresponded to the calculations carried out before the tests.

A series of experiments has been carried out to determine what happens in the event either of a catastrophic loss of vacuum or of a much smaller vacuum leak. A test facility was designed and assembled in which either of these scenarios could be investigated on a small scale. The test facility contained a 121 helium vessel, together with a system of valves, sensors and high-speed data acquisition. To carry out a test, the 121 vessel was filled with superfluid helium at 1.8 K. A fast-acting valve was then used to open a large hole in the insulating vacuum to simulate a

catastrophic leak, or a very small hole to simulate a small leak. By monitoring the rise of pressure and temperature, and the rate of change of mass of the vessel, the heat flux and venting rate could be calculated. These results can be extrapolated directly to the AMS-02 magnet, and have been used to qualify the cryogenic system for flight on the Space Shuttle.

In addition to these investigations, tests have also been carried out on prototype burst discs. Discs for protecting the vacuum tank have undergone vibration testing followed by controlled bursts. These tests have shown that the discs are not affected by the levels of vibration encountered during a launch. Further tests have been carried out on discs for protecting the helium vessel, which operate at 1.8 K. These discs have been shown to have extremely good leak tightness against superfluid helium.

### 3. The silicon tracker

The AMS-01 Silicon Tracker [9] was the first application in space of the high-precision silicon technology developed for position measurements in accelerator experiments [10]. The high modularity, low voltage levels ( $< 100$  V), and gas-free operation of the device is well suited to operation in space. The 1998 shuttle test flight demonstrated both the successful adaptation of the technology to the space environment and the feasibility of large area detectors. Silicon micro-strip sensors were originally developed for vertex detectors in colliding-beam experiments in order to provide a few high-precision position measurements near the interaction point. The AMS application differs considerably. The tracking information is provided uniquely by the silicon sensors, which implies a large surface area and higher inter-strip capacitances. The major challenges were to maintain the required mechanical precision and low-noise performance in the large-scale application, and to do so in outer space.

The silicon tracker is composed of  $41.360 \times 72.045 \times 0.300$  mm<sup>3</sup> double-sided silicon micro-strip sensors. The sensors have been produced at silicon foundries located in Switzerland [11] and Italy [12] using identical geometries and processing procedures. Over 4000 sensors have been produced to select the  $\sim 2500$  sensors of the very high quality required to assemble the Silicon Tracker units (ladders). Over  $2 \times 10^7$  electrical measurements have been performed using four automatic test stations. This large number of sensors makes the AMS Silicon Tracker the largest precision tracking detector ever built for a space application. Fig. 4 shows the principal elements of the silicon ladder and the main components of the readout hybrids.

The principal goals of the ladder fabrication are to guarantee the required precision for the relative alignment of the silicon sensors ( $< 5$   $\mu$ m), and minimize the degradation of the electrical performance due to handling and ultra-sonic bonding. Ladder fabrication was organized between three centres operating with identical procedures

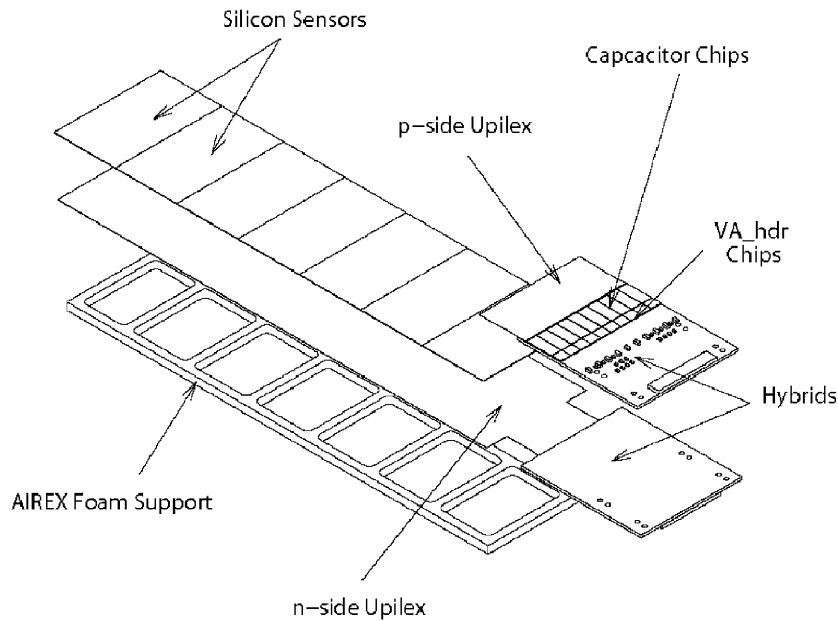


Fig. 4. The principal components of the silicon ladder.

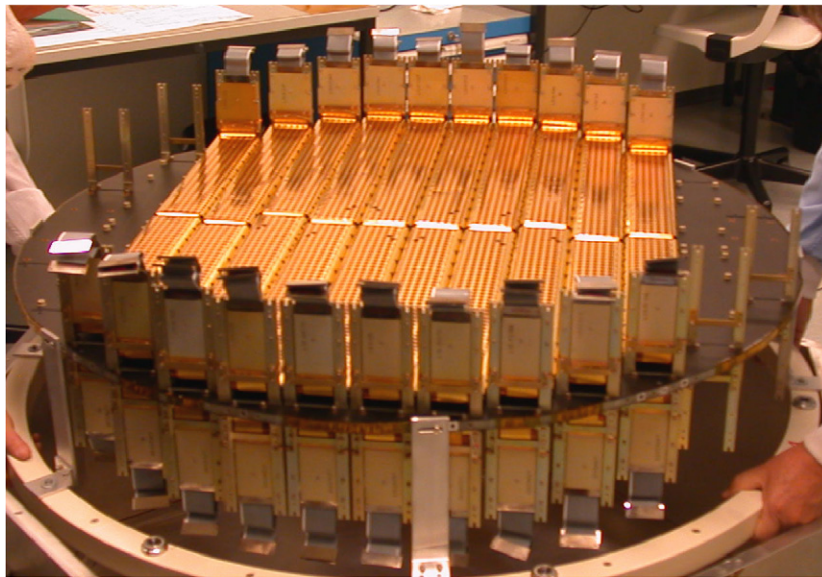


Fig. 5. Plane numbers 2 completely equipped with ladders.

derived from the AMS-01. During fabrication the sensor positions on a ladder are recorded with a 3D semi-automatic measuring machine. The results for the sensor alignment for the first 125 (out of 192) AMS-02 ladders are better than  $5\ \mu\text{m rms}$ .

The tracker support structure is divided into three sections: a carbon fibre cylindrical shell which supports the planes 2–4 located inside the magnet, and two carbon fibre flanges which support the exterior planes 1 and 5 [13]. With respect to the AMS-01 configuration, the number of silicon layers has been increased from 6 to 8 by suppressing one internal plane and equipping both sides of the remaining three internal planes with silicon ladders. When

ladders equipping a full tracker plane are produced, they are integrated onto the corresponding support plane. Supervision, quality control and traceability are ensured by a database developed for that purpose. The activities start with acceptance tests of the ladders arriving from all production lines and then proceed in steps toward integration of the complete detector. Installation of the second layer on the other side is more delicate since one has access from only one side for fixation. The assembled plane is finally stored in a light-tight container under dry nitrogen. Fig. 5 shows the first fully equipped inner plane.

The silicon sensors are grouped together, for readout and biasing, in ladders of different lengths to match the



cylindrical geometry of the AMS magnet. The maximum combined strip length in the silicon for a single readout channel is 60 cm. The relatively large input capacitance (30–180 pF), as well as the need for a high dynamic range (<100 MIPs), led to the development of a new front-end readout chip based on the low-noise Viking design, the VA\_hdr7 [14].

Each of the 64 channels of the VA\_hdr chip consists of a charge-sensitive amplifier, a CR-RC semi-Gaussian shaper, and a sample-and-hold stage. An analogue multiplexer, shift register and buffer are incorporated in the chip for sequential data output at a maximum clock frequency of 10 MHz. The equivalent noise charge as a function of capacitance load  $C_{det}$  has been measured to be  $(350 + 4C_{det}/pF) e^-$  at a  $6 \mu s$  peaking time and nominal bias currents. The VA\_hdr chips have an average power consumption 0.7 mW per channel. The single-channel response of the VA\_hdr chip has been measured to be linear up to  $\sim 75$  MIPs. The strips of the silicon sensors are ac-coupled to the VA\_hdr via 700 pF capacitor chips.

The hybrids are mounted on carbon fibre-metal cooling bars, which evacuate the heat generated by the front-end electronics inside the magnet. The presence of the superconducting magnet requires an active cooling system for the tracker. The AMS-02 Tracker Thermal Control System (TTCS) is a two-phase, mechanically pumped loop system. The cooling liquid,  $CO_2$  at about 80 bar pressure, is circulated by a pump. Outside of the tracker volume, the fluid passes through a heat exchanger to keep the incoming fluid just at the boiling point while minimizing the pre-heater power required. It is then directed to condensers on the tracker thermal wake and ram radiator panels facing deep space. There, the vapor-liquid mixture is cooled to below the boiling point, and then returns to the pump input, closing the circuit. Ammonia heat pipes embedded in the radiators increase their effectiveness. The relative flow of fluid to the wake and ram radiators is self-adjusting, the fluid will preferentially flow towards the cooler radiator.

Space-based particle detection systems have to cope with a far wider range of environmental conditions than those at

accelerators. This concerns notably the vibrations during the transport before deployment and the rapid periodic changes in the thermal settings due to solar radiation and cooling while in the shadow of Earth. With the AMS-02 silicon tracker, charged particle tracks are traced at 8 space points in a  $\sim 1 m^3$  sized B-field to an accuracy of better than  $10 \mu m$ . The alignment system provides optically generated signals in the 8 layers of the silicon tracker that mimic straight (infinite rigidity) tracks [15,16]. The AMS-02 tracker is equipped with  $2 \times 10$  pairs of alignment control beams. The beams are narrow (diameter  $< 0.5 mm$ ) and of small divergence ( $< 1 mrad$ ). The AMS approach to silicon tracker alignment control using IR laser beams fulfils the requirements of a space borne experiment. It is of light weight (3 kg), low power (1 mW), low dead time ( $< 1\%$ ) and provides a precision exceeding the tracker resolution ( $8 \mu m$ ) with less than 100 laser shots. The success of the AMS approach in Si tracker alignment control by IR laser beams has led the team building the largest Si tracker array [17] to develop a similar system for 10 years of operation at the LHC.

An extensive series of tests have been performed to verify the performance of the AMS-02 silicon tracker. For what concerns the spatial resolution the residual distributions of the ladder, described by a Gaussian function and flat background, they give widths of the Gaussians of 8.5 and  $30 \mu m$ , respectively, for the p- and n-sides. To study the AMS-02 ladder response to light and heavy ions, six ladders were exposed to an ion beam at CERN in October 2003. The tracker Z measurements are compared to those of prototype RICH detector in Fig. 6. An excellent correlation to the RICH Z measurement is seen for both side of the silicon sensors, namely K and S sides.

If compared to the precursor AMS-01 mission, the performance of the tracker in terms of signal to noise, position resolution and charge resolution have been greatly enhanced. The increase of silicon layers from 6 to 8, together with the more powerful AMS-02 cryomagnet, has significantly increased the physics reach of the AMS-02 detector, making a wide range of physical phenomena accessible during the AMS-02 mission.

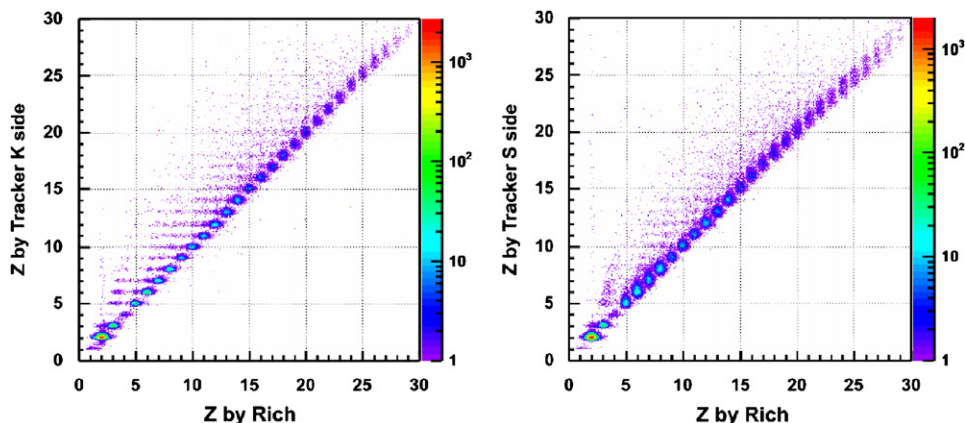


Fig. 6. Comparisons of charge ( $Z$ ) measurements by the Tracker and RICH.

#### 4. Conclusions

AMS-02 is the first precision particle physics experiment on the ISS. With its acceptance, resolution and ability to study different particles and nuclei over 3–5 years of data taking, it provides an opportunity to accurately explore new regions of physics.

#### Acknowledgements

The author thanks M. Capell for support during the preparation of this paper.

#### References

- [1] G. Jungman, et al., Phys. Rep. 267 (1996) 195;  
J.R. Ellis, et al., Nucl. Phys. B 214 (1998) 3;  
E.A. Baltz, J. Edsjo, Phys. Rev. D 59 (1999) 23511;  
T. Moroi, L. Randall, Nucl. Phys. B 570 (2000) 455.
- [2] P. Salati, et al., Nucl. Phys. Proc. Suppl. 81 (2000) 37.
- [3] A.D. Dolgov, Phys. Rep. 222 (1992) 309.
- [4] J.G. Asbury, et al., Phys. Rev. Lett. 18 (2) (1967) 65.
- [5] J.J. Aubert, et al., Phys. Rev. Lett. 33 (23) (1974) 1404.
- [6] For example, L3 Collaboration, Nucl. Instr. and Meth. A 289 (1990) 35.
- [7] B. Blau, et al., IEEE Trans. Appl. Supercond. 12 (2002) 349.
- [8] S. Harrison, et al., IEEE Trans. Appl. Supercond. 13 (2003) 1381–1384.
- [9] R. Battiston, Nucl. Phys. Proc. Suppl. 44 (1995) 274;  
J. Alcaraz, et al., Nuovo Cimento 112A (1999) 1325;  
W.J. Burger, Nucl. Phys. Proc. Suppl. 113 (2002) 139.
- [10] M. Acciarri, et al., Nucl. Instr. and Meth. A 351 (1994) 300;  
G.F. Dalla Betta, et al., Nucl. Instr. and Meth. A 431 (1999) 83.
- [11] S.A. Colibrys, Maladière 83, CH-2007 Neuchâtel.
- [12] ITC-irst; Via Sommarive 18, I-38050 Povo.
- [13] Oerlikon Contraves; Birchstrasse 155, CH-8050 Zürich.
- [14] IDE AS; Veritasveien 9, N-1323 Hovik.
- [15] J. Vandenhirtz et al., in: Proceedings of the 27th International Cosmic Ray Conference (ICRC2001), D-Hamburg, session OG, Vol. 5, 2001, p. 2197.
- [16] W. Wallraff et al., in: I-Villa Olmo Como, M. Barone et al. (Eds.), Proceedings of the Seventh International Conference on Advanced Technology and Particle Physics (ICATPP-7), World Scientific, Singapore, 2002, p. 149, ISBN:981-238-180-5.
- [17] Ostapchouk et al., 9 May 2001, CMS Note 2001/053, CMS–CERN.